

Car-Parrinello Molecular Dynamics With A Sinusoidal Time-Dependent Potential Field

Tobias Alznauer and Irmgard Frank*

Theoretische Chemie

Leibniz Universität Hannover

(Dated: May 29, 2022)

We solve the problem of applying an external field in periodic boundary conditions by choosing a sine potential. We present an implementation in the Car-Parrinello molecular dynamics code (CPMD) and discuss applications to electron and ion transfers in complex molecular systems.

Keywords: Density functional theory, Car-Parrinello molecular dynamics, external potentials

I. INTRODUCTION

Electrical fields may induce charge transport or also electrochemical reactions. To simulate such condensed-phase phenomena, it is desirable to have such an external field implemented in a code which allows to perform Car-Parrinello dynamics [1] using periodic boundary conditions [2]. The theoretical treatment of external fields within Kohn-Sham theory [3, 4] is in principle straightforward. The practical implementation in a code employing periodic boundary conditions, however, leads to the question how potential discontinuities of the potential energy at the borders of the unit cell should be treated. Several approaches to tackle this problem have been devised in the past years [5–10]. In the present paper we use a somewhat different approach with the aim to devise an implementation in the CPMD code which is both conceptually simple and simple to use in practical applications, even for time-dependent external fields. We achieve this by representing an external field by sine functions where the problem of discontinuities does not arise.

II. THEORETICAL BACKGROUND

Car-Parrinello molecular dynamics is based on an extended Lagrangian [1]

$$\mathcal{L} = \mu_e \sum_i \int |\dot{\psi}_i(\mathbf{r})|^2 d\mathbf{r} + \frac{1}{2} \sum_I m_I \dot{\mathbf{R}}_I^2 - E[\psi_i, \mathbf{R}] + \sum_i \sum_j \Lambda_{ij} \left(\int \psi_i^*(\mathbf{r}) \psi_j(\mathbf{r}) d\mathbf{r} - \delta_{ij} \right)$$

with the first two terms being the fictitious kinetic energy of the electrons and the kinetic energy of the nuclei, respectively, and the last term is the constraints resulting from the need to keep the orbitals orthogonal.

This results in the following equations of motion:

$$m_I \ddot{\mathbf{R}}_I(t) = -\frac{\partial}{\partial \mathbf{R}_I} E[\psi_i, \mathbf{R}] + \frac{\partial}{\partial \mathbf{R}_I} \{\text{constraints}\}$$

$$\mu_e \ddot{\psi}_i(t) = -\frac{\partial}{\partial \psi_i^*} E[\psi_i, \mathbf{R}] + \frac{\partial}{\partial \psi_i^*} \{\text{constraints}\}$$

The energy is calculated using the Kohn-Sham expression [3, 4]:

$$E[\psi_i, \mathbf{R}] = -\sum_i \frac{1}{2} \int \psi_i^*(\mathbf{r}) \nabla_i^2 \psi_i(\mathbf{r}) d\mathbf{r} + \sum_{I < J} \frac{Z_I Z_J}{|\mathbf{R}_I - \mathbf{R}_J|} - \sum_I \int \frac{Z_I \rho(\mathbf{r})}{|\mathbf{R}_I - \mathbf{r}|} d\mathbf{r} + \frac{1}{2} \iint \frac{\rho(\mathbf{r}) \rho(\mathbf{r}')}{|\mathbf{r} - \mathbf{r}'|} d\mathbf{r} d\mathbf{r}' + E_{xc}[\psi_i] \quad \text{with } \rho(\mathbf{r}) = \sum_i \int \psi_i^*(\mathbf{r}) \psi_i(\mathbf{r}) d\mathbf{r}$$

We add the time-dependent external potential to the Kohn-Sham energy expression:

$$E_t[\psi_i, \mathbf{R}] = E[\psi_i, \mathbf{R}] + \sum_I \int \frac{Z_I v_{\text{sine}}(\mathbf{r}', t)}{|\mathbf{R}_I - \mathbf{r}'|} d\mathbf{r}' - \iint \frac{v_{\text{sine}}(\mathbf{r}', t) \rho(\mathbf{r})}{|\mathbf{r} - \mathbf{r}'|} d\mathbf{r}' d\mathbf{r}$$

We have implemented into the Car-Parrinello molecular dynamics code [2] a sinusoidal potential field which may change temporally and spatially in three dimensions. For one spatial dimension:

$$v_{\text{sine}}(x, t) = (a(t) + A) \cdot \sin\left(2\pi \frac{x}{l_x} + b(t)\right)$$

$a(t)$ and $b(t)$ may be linear or sinusoidal functions. With this flexible implementation, a broad range of phenomena can be simulated. However, it must be considered that the wave length cannot exceed the size of the unit cell as the spatial part $2\pi x/l_x$ ensures that the periodic boundary conditions are fulfilled.

* <http://www.theochem.uni-hannover.de/>;
irmgard.frank@theochem.uni-hannover.de

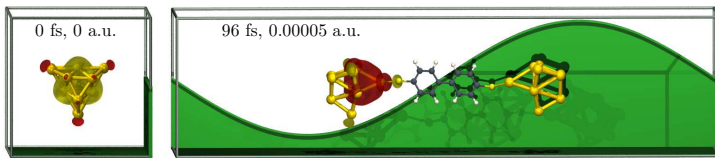


FIG. 1. Arrangement of the gold-dibenzenedithiol-gold junction in the supercell. (grey: C, white: H, yellow: S, gold: Au)

III. APPLICATIONS

A. Electron Motion: Time-Dependent Amplitude

Metal-molecule-metal junctions are used to measure the electron transport across single molecules. Many experimental and theoretical studies aimed at understanding the mechanism of the electron transport (see [11] and literature cited therein). It was found that the resulting current depends on many factors which are difficult to define experimentally. In particular the precise arrangement of a single molecule between two surfaces or tips is not easy to control in experiment. Most of the molecules under investigation are isolators and the distance between the surfaces or tips is in the order of a nanometer, hence one may ask the question if the effective current is significantly influenced by the linking molecules. In an early study [12] of tunneling through a C_{60} molecule currents in the order of 10^3 nA were found at a voltage of 0.05 V which decrease by several orders of magnitude if the tip-surface distance was increased above 10 \AA . A better electronic connection is obtained if the molecule is covalently linked to one or both surfaces. In a study of a self-assembled monolayer on a gold surface [13] a switching between an ON and an OFF state of organic molecules was observed. It was characterized by the temporally changing apparent heights of the organic layer (between 1 and 4 \AA) at an applied voltage of -1.4 V and a tunneling current in the order of 10^{-4} nA. The dependence of the tunneling current on covalent anchoring was studied in [14]. Depending on the bonding situation and on the thickness of the organic layer, current densities between 10^{-7} and 10^{-2} A/cm² were measured for voltages above 0.5 V. Theoretical investigations were usually performed using perturbation theory approaches or studying the density of states obtained from density functional calculations [11, 15, 16]. Direct dynamics calculations with an explicit external field give a more complete picture of the full time evolution of a complex system. In the present study we want to illustrate the influence of a three-dimensional electrical field on a metal-molecule-metal junction.

We studied a system consisting of a dibenzenedithiol molecule covalently linked to two gold clusters. The electric field is applied along the junction (Figure 1).

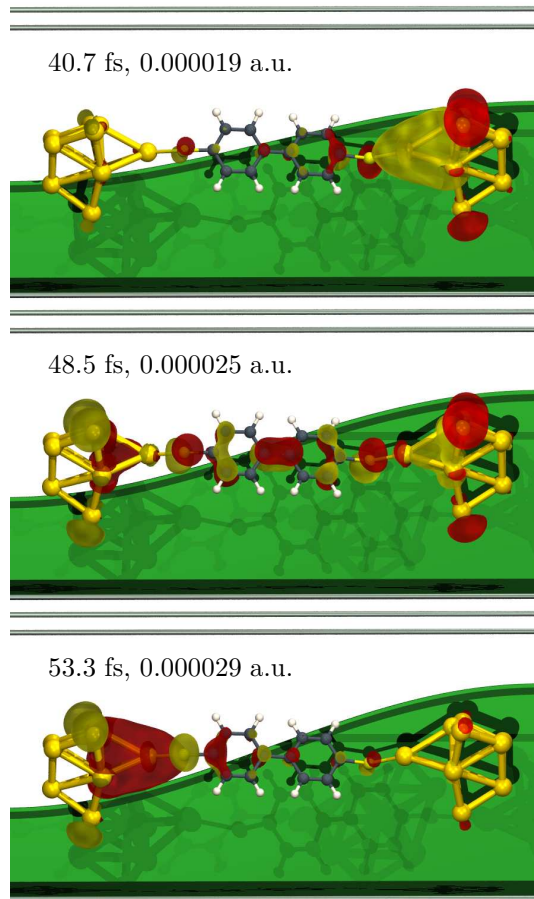


FIG. 2. Snapshots of the motion of a localized orbital during the application of an external field with increasing amplitude to a gold-dibenzenedithiol-gold junction.

A field with the following parameters was used: $A=0.000025$ a.u., $a(t)=0.000025 \cdot \sin\left(\frac{2\pi}{193.5 \text{ fs}} \cdot t - \frac{\pi}{2}\right)$ a.u., $b(t)=0$.

The amplitude varies sinusoidal with time between 0 and 0.00005 a.u. (0.03 kcal/mol, ≈ 1.4 kV/mm). The transfer of one electron along the molecular junction is observed.

The snapshots in Figure 2 show the motion of a localized (Wannier) orbital. The orbital coefficients at the gold cluster at the right side of the figure decrease and density is transferred to the aromatic system. Within about 10 fs the transfer to the opposite cluster is completed. Even if the motion of individual spin orbitals is observed, in total the spin effects cancel and the total spin density (not shown) is essentially zero during the full process. The external field causes a shift of the total charge rather than a build-up of spin density. This shift occurs in a continuous motion. The total many-electron density is just slightly shifted to one side.

Figure 3 shows the course of the energies and the temperature during the simulation run. The total energy is raised by about 40 kcal/mol due to the application of

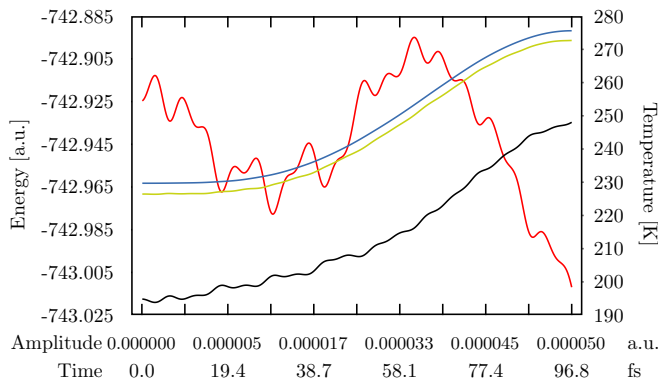


FIG. 3. Total energy of the Car-Parrinello Lagrangian (blue), energy of the classical Hamiltonian (green), Kohn-Sham energy (black), temperature (red) during the application of an external field to a gold-dibenzenedithiol-gold junction.

the external field.

The electrons follow essentially instantaneously even if the fictitious mass of the electrons is high in Car-Parrinello molecular dynamics simulations which results in a slower electronic motion compared to experiment. The process is essentially adiabatic and is determined by the change of the amplitude of the external field. These first results indicate that the influence of the chemical nature of the junction on the current is small due to the small metal-metal distance. However, the intermediate build-up of orbital density in the aromatic system shows that it is different from zero, the aromatic system takes actively part in the charge transfer.

B. Ion Migration: Time-Dependent Phase

β -Eucryptite (LiAlSiO_4) [17] is known as a one-dimensional Li^+ ionic conductor, a substance class which is of high interest for the development of batteries [18, 19]. For a similar material, $\text{Li}_7\text{La}_3\text{Zr}_2\text{O}_{12}$, an unusual concerted mechanism for ion migration has been found in a recent theoretical study using first principles equilibrium simulations at high temperatures [20]. In β -eucryptite the conductivity is along the crystallographic c -axis of the quartz-like structure. To study the migration of the ions in the crystal, a system is modeled with one crystal defect introduced in the supercell (Figure 4). A Li^+ ion is removed and a Si^{4+} ion is substituted by an Al^{3+} ion to obtain a neutral system. The potential field is applied along the c -axis. The phase of the potential field varies linearly in time.

A field with the following parameters was used: $A=0.0001$ a.u., $a(t)=0$, $b(t)=\frac{2\pi}{483.8 \text{ fs}} \cdot t$. The field which has an amplitude of 0.0001 a.u. (0.06 kcal/mol, ≈ 3.6 kV/mm) is moving with a velocity of 15000 m/s, respec-

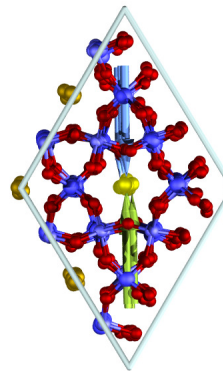


FIG. 4. Unit cell of β -eucryptite. Within the unit cell the lithium ions may migrate along four different channels. Dark blue: Si, blue: Al, red: O, gold: Li, yellow: Li channel with vacancy. Only in this channel Li motion is observed.

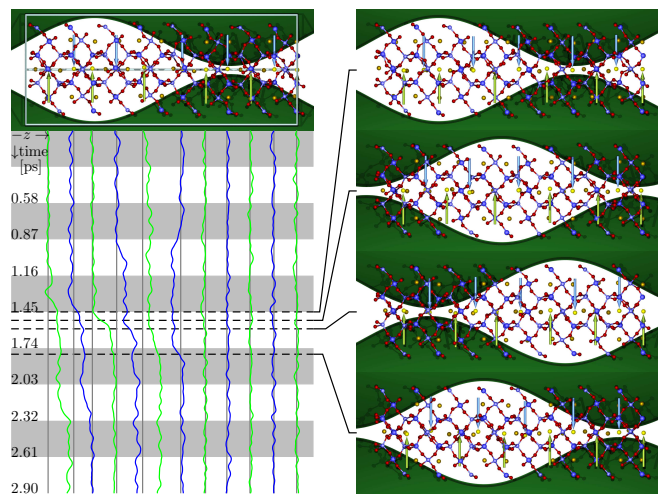


FIG. 5. Snapshots from a CPMD simulation showing the motion of lithium ions (yellow) in β -eucryptite. The channel containing a vacancy is shown in light yellow. Dark blue: Si, blue: Al, red: O. The arrows mark the migrating lithium ions. The migration can also be followed from the trajectories to the left. Five lithium ions in the left half of the simulation cell shown migrate to the next lattice site generating a new vacancy at the left border of the simulation cell.

tively. This corresponds to a phase shift of 2π within 0.29 ps. The series of snapshots in (Figure 5) shows the migration of five Li^+ -ions to new lattice sites on a time scale of a few hundred femtoseconds as indicated by the moving arrows. The motion is started by a lithium ion near the left border of the simulation cell. The neighbouring lithium ions follow till the original vacancy is filled and a new vacancy near the left border of the simulation cell is generated. On a longer time scale this vacancy would be filled by lithium ions from the right border (respecting periodic boundary conditions).

In Figure 6 the temporal evolution of the energies and

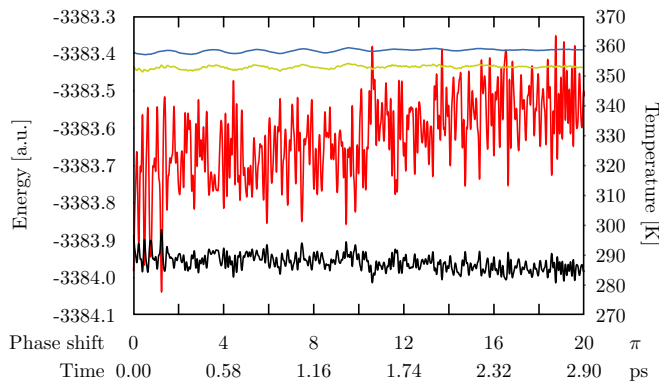


FIG. 6. Total energy of the Car-Parrinello Lagrangian (blue), energy of the classical Hamiltonian (green), Kohn-Sham energy (black), temperature (red) during the application of a temporally moving external field to β -eucryptite.

temperature is shown. The total energy shows a slight oscillation in the beginning when the field is turned on. The kinetic energy of the electrons (difference between the total energy and the energy of the classical Hamiltonian) stay small. The temperature (corresponding to the difference between the energy of the classical Hamiltonian and the Kohn-Sham energy) shows a slight increase by about 30 K. The ion migrations are possible with a rather moderate take-up of energy.

IV. CONCLUSIONS

We have added a sinusoidal field to Car-Parrinello molecular dynamics. The field can change with phase and amplitude. Like this it is possible to model a vast diversity of experimental situations in which an electrical field matters. In principle, the approach can be extended to more complex periodic fields by using more than one sine function. In first applications we have illustrated the

application to electron and ion transfers. For a metal-molecule-metal junction we find that the electrons follow the electric field nearly adiabatically along the junction. For a lithium ion conductor we find a consecutive hopping of ions to neighbouring lattice sites along a channel containing a defect. The method is quantitative in principle, however, the simulations are limited to periodic fields with wave lengths not larger than the unit cell lengths and to time scales which allow for very fast changing fields only. Being able to follow the complex electronic and ionic motion is the main advancement from such first-principle calculations. The simulations may serve as a check if simpler models are applicable.

V. METHODS

The simulations were performed using Car-Parrinello molecular dynamics [1] as implemented in the CPMD plane wave code [2]. For all calculations the BLYP exchange-correlation functional [21, 22] was used in its unrestricted formulation (LSD). Troullier-Martins pseudopotentials were employed for describing the core electrons [23]. The pseudopotential cutoff was set to 70.0 Rydberg. The fictitious electron mass was set to 400 a.u. and a time step of 4 a.u. (0.097 fs) was used. After the equilibration, the temperature was not controlled. For the simulations of the metal-molecule-metal junctions a periodically repeated simulation cell with a size of $15 \times 15 \times 60 \text{ \AA}^3$ was used. The systems were initially equilibrated at a temperature of 150 K in order to reduce molecular vibrations and to focus on the electronic motion.

For the simulations of the eucryptite crystal periodic boundary conditions were applied with a cell size of $10.5 \times 9.1 \times 44.8 \text{ \AA}^3$. The systems were equilibrated at 300 K.

VI. ACKNOWLEDGEMENTS

We thank Marius Schulte for helpful discussions.

-
- [1] R. Car and M. Parrinello, *Phys. Rev. Lett.* **55**, 2471 (1985).
 - [2] CPMD, CPMD, Version 3.15, J. Hutter et al., <http://www.cpmc.org/>, Copyright IBM Corp 1990-2008, Copyright MPI für Festkörperforschung Stuttgart 1997-2001.
 - [3] P. Hohenberg and W. Kohn, *Phys. Rev. B* **136**, 864 (1964).
 - [4] W. Kohn and L. J. Sham, *Phys. Rev. A* **140**, 1133 (1965).
 - [5] K. N. Kudin, R. Car, and R. Resta, *J. Chem. Phys.* **126**, 234101 (2007).
 - [6] K. N. Kudin, R. Car, and R. Resta, *J. Chem. Phys.* **127**, 194902 (2007).
 - [7] M. Springborg and B. Kirtman, *J. Chem. Phys.* **126**, 104107 (2007).
 - [8] M. Springborg and B. Kirtman, *Phys. Rev. B* **77**, 045102 (2008).
 - [9] M. Springborg and B. Kirtman, *Phys. Rev. E* **77**, 209901 (2008).
 - [10] B. Kirtman, M. Ferrero, M. Rérat, and M. Springborg, *J. Chem. Phys.* **131**, 044109 (2009).
 - [11] Q. Sun, A. Selloni, and G. Scoles, *J. Phys. Chem. B* **110**, 3493 (2006).
 - [12] C. Joachim, J. K. Gimzewski, R. R. Schlittler, and C. Chavy, *Phys. Rev. Lett.* **74**, 2102 (1995).
 - [13] Z. J. Donhauser, B. A. Mantooth, K. F. Kelly, L. A. Bumm, J. D. Monell, J. J. Stapleton, D. W. Price, A. M. Rawlett, D. L. Allara, J. M. Tour, and P. S. Weiss, *Science* **292**, 2303 (2001).
 - [14] Y. Selzer, A. Salomon, and D. Cahen, *J. Phys. Chem. B* **106**, 10432 (2002).

- [15] C. Joachim, J. K. Gimzewski, and A. Aviram, *Nature* **408**, 541 (2000).
- [16] S. Piccinin, A. Selloni, S. Scandolo, R. Car, and G. Scoles, *J. Chem. Phys.* **119**, 6729 (2003).
- [17] U. V. Alpen, E. Schönherr, H. Schulz, and G. H. Talat, *Electrochimica Acta* **22**, 805 (1977).
- [18] R. Murugan, V. Thangadurai, and W. Weppner, *Angew. Chem.* **46**, 7778 (2007).
- [19] H. Buschmann, J. Dölle, S. Berendts, A. Kuhn, P. Böttke, M. Wilkening, P. Heitjans, A. Senyshyn, H. Ehrenberg, A. Lotnyk, V. Duppel, L. Kienle, and J. Janek, *Phys. Chem. Chem. Phys.* **13**, 19378 (2011).
- [20] R. Jalem, Y. Yamamoto, H. Shiiba, M. Nakayama, H. Munakata, T. Kasuga, and K. Kanamura, *Chem. Mater.* **25**, 425 (2013).
- [21] A. Becke, *Phys. Rev. A* **38**, 3098 (1988).
- [22] C. Lee, W. Yang, and R. G. Parr, *Phys. Rev. B* **37**, 785 (1988).
- [23] N. Troullier and J. L. Martins, *Phys. Rev.* **43**, 1993 (1991).